Alexandria Journal of Medicine (2011) **47**, 1–9

Alexandria University Faculty of Medicine

Alexandria Journal of Medicine

www.sciencedirect.com

REVIEW ARTICLE

Plasmonic photo-thermal therapy (PPTT)

Xiaohua Huang [a], **Mostafa A. El-Sayed** [b,*]

[a] *Department of Chemistry, University of Memphis, Memphis, TN 38152, United States*
[b] *School of Chemistry and Biochemistry, Georgia Institute of Technology, Atlanta, GA 30332, United States*

Received 2 October 2010; accepted 1 January 2011

KEYWORDS

Gold nanoparticles;
Cancer;
Photo-thermal therapy;
Hyperthermia;
Surface plasmon resonance

Abstract Photo-thermal therapy (PTT) is a minimally-invasive therapy in which photon energy is converted into heat to kill cancer. Gold nanoparticles absorb light strongly and convert photon energy into heat quickly and efficiently, thereby making them superior contrast agents for PTT. This gold nanoparticle-assisted PTT called PPTT has showed great popularity and success in recent years. The present review starts with the outline of optical properties that base PPTT followed by description of the synthesis of several gold-based nanoparticles that have been used in PPTT including gold nanospheres, gold nanoshells, gold nanorods and gold nanocages. Therapeutic outcomes will be discussed for each type of gold nanoparticles. Cell death mechanisms and future perspectives of PPTT will be briefly mentioned at the end.

Contents

* Corresponding author. Tel.: +1 404 894 4002.
E-mail address: melsayed@gatech.edu (M.A. El-Sayed).

2090-5068

Peer review under responsibility of Alexandria University Faculty of Medicine.
doi:10.1016/j.ajme.2011.01.001

Production and hosting by Elsevier

1. Introduction

Cancer is a disease characterized by uncontrolled growth and spread of abnormal cells. It is caused by DNA damage which can be inherited or induced by environmental factors. Cancer can form tumors on tissues or grow in the body flow system. In the United States, cancer and heart attack compete in being the number one killers of humans, with 1,479,350 new cases of cancer and 562,340 deaths estimated in 2009.[1]

Current mainstream treatments include surgery, chemotherapy or radiation. Surgical extirpation is highly effective in primary tumors, but it is limited to surgically recognizable and accessible tumors and thus cancer cells may not be completely removed. Chemotherapy is the use of chemical drugs to fight cancer. The systemically administrated drugs circulate in the body to kill cells that divide rapidly, especially cancer cells. It commonly has significant side effects due to the drug toxicity to normal cells and is subject to the development of resistance by the cancer cells. Radiation, the use of high energy ionization particles (X-rays, gamma rays or electrons) to damage cell and tissue at a molecular level, is often used as a complementary approach, to eradicate remaining cancer cells after surgery. It can cause damage to the healthy tissues close to the cancer cells or in the path of the radiation beam.

Photo-thermal therapy (PTT), a minimally-invasive therapeutic strategy in which photon energy is converted into heat sufficient to destroy cancer cells, has been used to treat cancer to some degree in the past few decades.[2] Heating sources including near infrared or visible light, radiofrequency waves, microwaves, and ultrasound waves are used to induce moderate temperature rise in a specific target region to destroy the cancer cells, clinically termed as hyperthermia. Due to low absorption efficiency of the natural tissue absorbents, synthetic organic dye molecules, such as indocyanine green, naphthalocyanines and porphyrins coordinated with transition metals are externally administrated into the tumor sites to enhance the photothermal effects. As the dye molecules photobleach quickly, PTT has not been widely used in clinical settings.

Recently PTT has attracted new interest in the battle against cancer because of the generation of a novel class of photothermally sensitized agents – nanoscale gold. Gold metal at the nano-scale (billionths of a meter) shows superior light absorption efficiency over conventional dye molecules. Upon irradiation to electromagnetic radiation, strong surface fields are induced due to the coherent excitation of the electrons in the nanogold. The rapid relaxation of these excited electrons produces strong localized heat capable of destroying surrounding targeted cancer cells via hyperthermia or other thermal-based effects. This photothermal therapy induced by plasmonic gold nanoparticles is called plasmonic photothermal therapy (PPTT).[3] In this chapter, we will give an overview of the gold nanotechnology-driven photothermal cancer therapy including a discussion of the optical properties, synthesis, therapeutic outcomes and insights into cell death mechanisms.

2. Optical properties of gold nanoparticles

2.1. Localized surface plasmon resonance

Compared to non-metal nanoparticles, plasmonic nanoparticles hold a unique photophysical phenomenon, called localized surface plasmon resonance (LSPR) (Fig. 1A).[4] This LSPR is the result of the interaction of nanoparticles with light of resonant frequency. As a result of the absorption of resonant light, the free electrons of the metal exhibit a collective coherent oscillation around the nanoparticle surface. This coherent oscillation induced as a result of the absorption of light in resonance with the incident light is called the localized surface plasmon resonance. This plasmon resonance leads to a strong extinction band around 520 nm in the visible spectral region, which is the reason for the brilliant red color of the nanogold solution. Back in 1908 Gustav Mie[5] theoretically explained this phenomenon by solving Maxwell equations. For nanoparticles much smaller than the wavelength of the light (~25 nm), the dipole oscillation is dominant and the extinction cross section is simplified to the following well known expression (Eq. (1)).

$$C_{\text{ext}} = \frac{24\pi^2 R^2 \varepsilon_{\text{m}}^{3/2}}{\lambda} \frac{\varepsilon_{\text{i}}}{(\varepsilon_{\text{r}} + 2\varepsilon_{\text{m}})^2 + \varepsilon_{\text{i}}^2} \quad (1)$$

where C_{ext} is the extinction cross section, R is the radius of the particle, λ is the wavelength of the incident light, ε_{m} is the dielectric constant of the surrounding medium, ε is the complex dielectric constant of the metal given by $\varepsilon =$

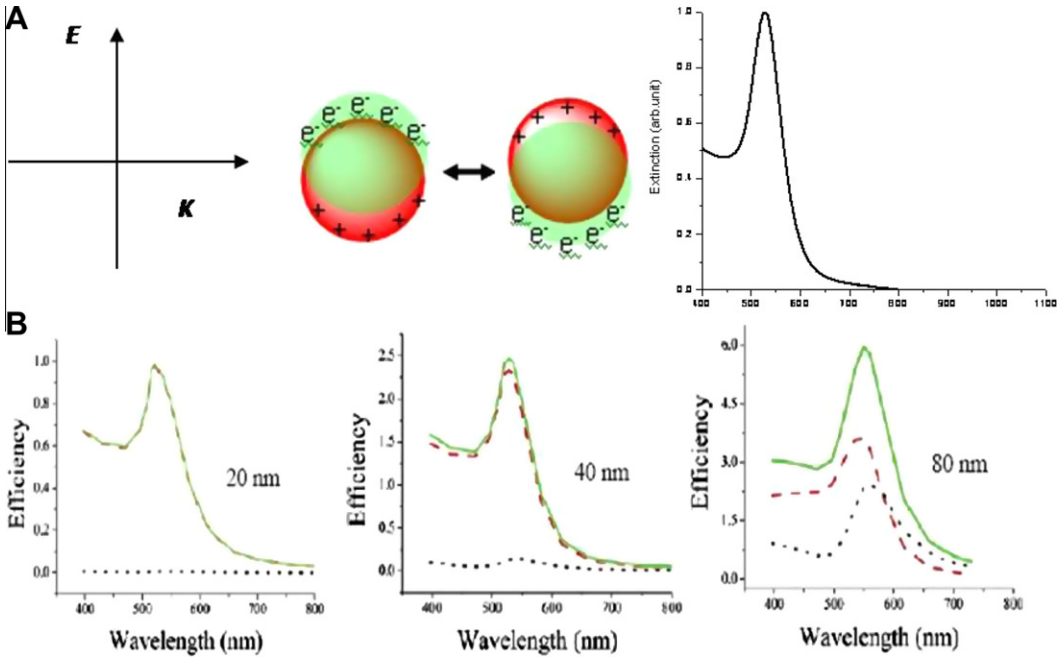

Figure 1 Schematic illustration of localized surface plasmon resonance (A) and calculated absorption and scattering properties of gold nanoparticles in different sizes (B). The electric field of incident light induces coherent collective oscillation of conduction band electrons with respect to the positively charged metallic core. This dipolar oscillation is resonant with the incoming light at a specific frequency that depends on particle size and shape. The absorption and scattering efficiencies depend on the size of the nanoparticles. Increasing nanoparticle size leads to an increase of light scattering contribution. (A) Reproduced with permission from Huang et al.[4]; (B) reproduced with permission from Jain et al.[6]

$\varepsilon_r(\omega) + i\varepsilon_i(\omega)$. The real part of the dielectric constant of the metal determines the SPR position and the imaginary part determines the bandwidth. The SPR resonance occurs when $\varepsilon_r(\omega) = -2\varepsilon_m$. For larger nanoparticles, full Mie theory has to be used to explain the LSPR considering all multiple electron oscillations.

The LSPR is dependent on factors affecting the electron charge density on the particle surface, such as the particle size, shape, structure, and the dielectric properties of the metal and the surrounding medium. Spherical gold, silver, and copper nanoparticles have strong SPR band in the visible region, while other metals show broad and weak bands in the UV region. Hollow or core-shell structures show a very red shifted band of the LSPR wavelength compared to the solid structures. Anisotropic nanoparticles, such as rods, triangles, and branched structures also exhibit a red shifted SPR band compared to their spherical analogs.

2.2. Optical absorption and scattering

The total loss of light interacting with plasmonic nanoparticles, i.e., the extinction, is a sum of absorption and scattering. Light absorption results when the photon energy is dissipated due to inelastic processes. Light scattering occurs when the photon energy causes electron oscillations in the matter which emit photons in the form of scattered light at the same frequency as the incident light. The contribution of these two parts to the total extinction can be calculated by using Mie theory or discrete dipole approximation (DDA). Fig. 1B shows calculated absorption, scattering and extinction efficiencies of gold nanoparticles in different sizes by using the full Mie theory.[6] For small nanoparticles, the extinction is dominated by absorption. Increasing nanoparticle size significantly increases light scattering.

In noble metal nanoparticles, both the absorption and scattering efficiencies are strongly enhanced due to the LSPR. The light absorption or scattering of gold nanoparticles is at least 1000 times stronger than the absorption or emission of any organic dye molecules. This makes gold nanoparticles very promising in a wide range of applications including sensing, imaging and photo-thermal therapy.

2.3. Tuning LSPR to NIR region

By changing the structure and shape, the LSPR frequency of gold nanoparticles can be tuned to near infrared (NIR) region, where light penetration in tissue is optimal. For this reason, NIR-absorbing gold-based nanoparticles have received considerable attention in PPTT.

Currently there are three major types of NIR-absorbing gold-based nanoparticles that are useful in PPTT (Fig. 2): gold nanoshell (Au NS),[7] gold nanorod (Au NRs)[4] and gold nanocage (Au NCs).[8] Au NS is composed of a spherical silica core (100–200 nm in diameter) and a thin layer of gold (5–20 nm). Its NIR absorption is firstly predicted by Neeves and Birnboim in 1989[9] and then experimentally validated by Halas and co-workers in 1998.[10] This two concentric spherical structures shows red-shifted absorption due to the coupling between the inner and outer shell surface plasmons.[11] Decreasing the ratio of shell thickness to core radius largely red shifts the LSPR wavelength from the visible to NIR region. As shown in Fig. 2, the LSPR wavelength

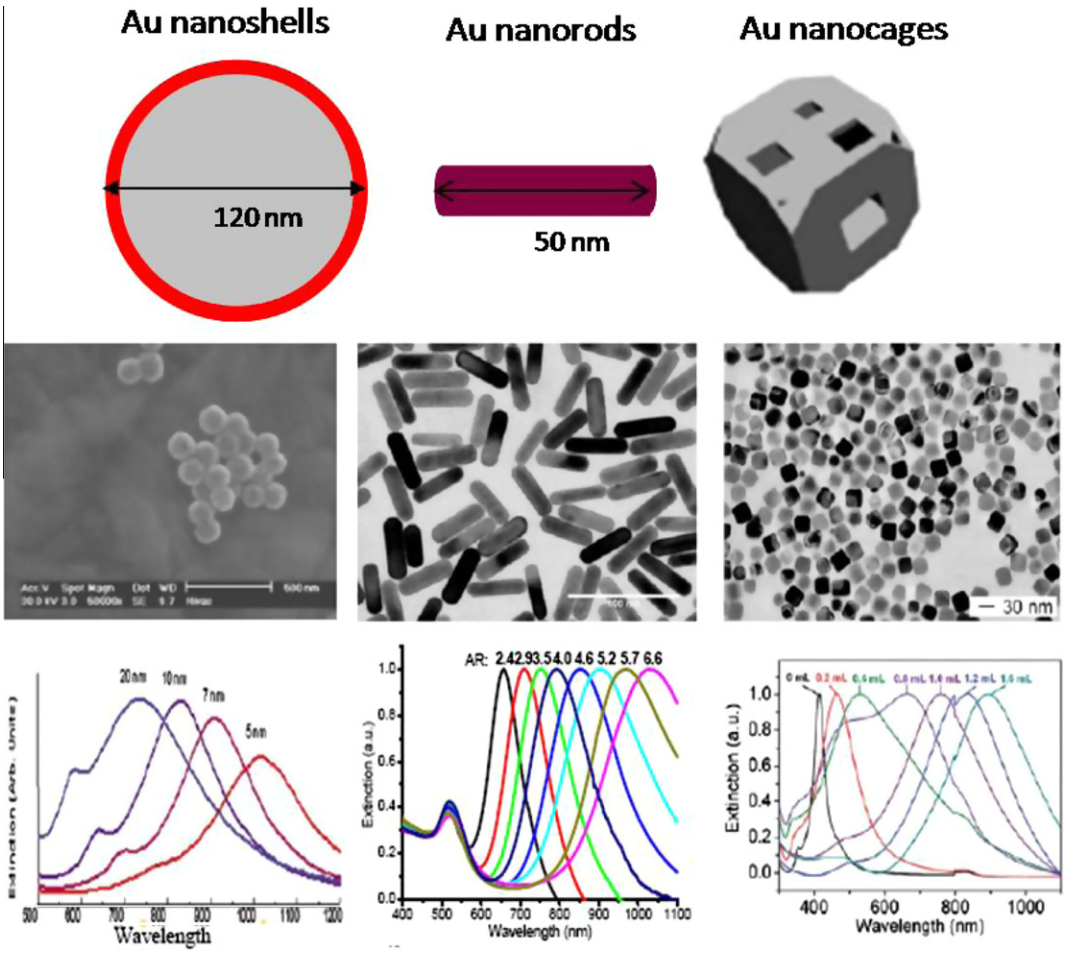

Figure 2 NIR-absorbing Au NPs in PPTT of cancer. Left column: Au NSs. Reproduced with permission from Loo et al.[7]; Middle column: Au NRs. Reproduced with permission from Huang et al.[4]; Right column: Au NCs. Reproduced with permission from Hu et al.[8]; First row: schematic illustration of the structures of Au NSs, NRs and NCs; Second row: TEM images; Third row: surface plasmon extinction spectra. The surface plasmon band is tuned to the NIR region by changing the shell to core ratio, the aspect ratio and the particle size, wall thickness and wall porosity for Au NSs, NRs and NCs, respectively.

shifts from 700 to 1000 nm when the shell thickness decreases from 20 to 5 nm. The LSPR frequency decreases near-exponentially with decrease in the shell thickness-to-core radius ratio, with a trend that is universal and independent of the nanoshell size, core material, shell metal, or surrounding medium.[12]

Developed by Wang,[13] Murphy[14] and El-Sayed[15] groups, Au NR has gained considerable popularity in various applications due to their precisely and readily controlled NIR optical properties. The cylinder shaped Au NR shows two absorption bands: a strong absorption band in the NIR region due to the electron oscillation along the longitudinal direction and a weak band in the visible region around 520 nm due to electron oscillation along the transverse direction. This optical behavior has been well explained using Gans theory.[16] The transverse band is insensitive to the aspect ratio (length/width) of the rod. The longitudinal band wavelength greatly red shifts from visible to NIR region in a linear relationship with increased intensity when the aspect ratio increases.[17] The LSPR wavelength is red shifted from 640 to 1050 nm by simply changing the aspect ratio from 2.4 to 6.6 (Fig. 2). Compared to nanoshells, DDA calculation shows that nanorods show 2–3 times stronger absorption efficiency.[8] Their physical dimension is also much smaller than the nanoshells.

Compared to Au NS and NR, Au NC is developed as a NIR-absorbing gold nanostructure by Xia group.[18] It is composed of a thin and porous gold wall with hollow interior. Changing the wall thickness, the hole size and porosity can tune the LSPR wavelength from the visible to the NIR region. This is experimentally controlled by the amount of auric acid that galvanically replaces silver cubes to obtain the nanocages.[18] Increasing the amount of the auric acid red shifts the LSPR (Fig 2). DDA calculation shows a 2 nm decreasing of the wall thickness cause a red shift of the LSPR wavelength by about 100 nm.[19] Increasing the polarity does not influence the position of the LSPR band, but significantly decreases the intensity in a linear way.

2.4. Photo-thermal properties

The PPTT rationale is that plasmonic nanoparticles have useful non-radiative photo-thermal properties. The absorbed

light is converted into heat through a series of photo-physical processes.[20] Firstly, the absorbed light is quickly converted to heat to form a hot metallic lattice by two processes: electron-electron relaxation occurring on femto-seconds and electron-phonon relaxation occurring on the picoseconds. Hot electron temperatures of several thousand degree kelvin are easily reached in the nanoparticles even with laser excitation powers as low as 100 nJ and the lattice temperature on the order of a few tens of degrees can be achieved. The lattice then cools off by phonon–phonon relaxation. It means the heat is dissipated from the particles into the surrounding environment to heat up the species surrounding the nanoparticles. When the nanoparticles are attached to cancer cells, the heat can change the function of the cells and even destroy them depending on the amount of heat generated by the hot nanoparticles.

Such fast energy conversion and dissipation can be readily used for the heating of the local environment by using light radiation with a frequency strongly overlapping with the nanoparticle SPR absorption band. For sufficient heating, relatively modest continuous laser light is generally used. Depending on the LSPR wavelength, the laser light is either in the visible region using spherical gold nanoparticles or in the near infrared (NIR) region using NIR-absorbing gold-based nanoparticles. For in vivo applications, NIR PPTT is favorable as the NIR light penetrates tissue optimally due to minimal absorption by the major absorbents of water and hemoglobin in the tissue. Thus Au NSs, NRs, and NCs have been actively investigated for their potentials in PPTT of cancer.

3. Nanoparticle synthesis

3.1. Gold nanospheres

Modern synthesis of visible-absorbing gold nanoparticles dates back to 1857 when Faraday made the colloid gold by reducing auric acid with phosphors.[21] Current popular method for making colloid gold was developed by Turkevich et al. in 1951[22] and later modified by Frens in 1973,[23] named as citrate reduction method. In this method, sodium citrate reduces auric acid at 100 °C to form nanoparticles. The negatively charged citrate also binds to the nanoparticles and stabilizes them in the solution phase. Changing the amount of sodium citrate makes nanoparticles of different sizes from a few to over a hundred nanometers. Some other methods include Schmid method,[24] Brust–Schiffrin method[25] and seed-mediated growth method.[26]

3.2. Gold nanoshells

Au NSs were developed by Halas group in 1997.[10] Silica nanoparticles around 120 nm in diameter are firstly prepared by Stöber method in which tetraethyl orthosilicate is reduced by ammonium hydroxide. The nanoparticles are laminated with amino-propyltriethoxysilane and then coated with small gold nanoparticles by covalent interaction. A uniform shell of gold is formed by depositing more gold onto the gold seed layer in the presence of auric acid and reducing agent of sodium borate. The concentration of auric acid determines the shell thickness. It is noticed that precise controlling of the metallic shell thickness, coverage and smoothness is challenged because of the instability of gold cluster and the difficulty of deposition of metal atoms onto the silica core. Nonetheless, this method is regarded as the general way to synthesize dielectric metal nanoshell structures.

3.3. Gold nanorods

High yields of gold nanorods suspension were firstly prepared by the electrochemical method developed by Wang and co-workers in 1990s.[13] A gold metal plate anode, a platinum plate cathode and a silver plate are immersed in an electrolytic solution consisting of a rod inducing CTAB surfactant and a co-surfactant TOAB (tetradodecylammonium bromide). The gold metal is electrolyzed to generate gold ions which then migrate to the cathode where they are reduced to gold atoms to form nanorods. The aspect ratio of the nanorods is controlled by the concentration and the release rate of silver ions produced from the redox reaction between gold ion and silver plate. Later, a seed mediated growth method was developed by Murphy group[14] and later modified by El-Sayed group.[15] This method has turned out to be the most popular method for making colloidal gold nanorods on account of their simplicity of the procedure, high quality and yield of nanorods, ease of particle size controlling and flexibility for structural modifications. This method involves two steps: In the first step, 2–5 nm gold nanospheres are prepared as seed NPs by the reduction of auric acid with sodium borate. In the second step, a bulk gold solution in the presence of CTAB surfactant and silver ions is reduced to Au^{+1} solution by ascorbic acid. To this growth solution, the seed NPs are introduced and NRs are formed within 2 h by anisotropic growth from the sphere NPs. The nanorods are capped by the CTAB molecules in a bilayer structure. The aspect ratio is controlled by the amount of silver ions with increasing amount of silver for higher aspect ratios. The use of a co-surfactant BDAC (benzyldimethylhexadecylammonium) facilitates the growth of nanorods of higher aspect ratios.

One other method for making monodisperse Au NRs is the earlier reported hard template method,[27] in which nanorods are grown in a nanoporous solid template and then dispersed in an aqueous or organic solvent to form nanorods solution. Photochemical reduction,[28] X-ray irradiation,[29] proton beam irradiation,[30] microwave reduction[31] and solvothermal reduction[32]can also make nanorods with good quality.

3.4. Gold nanocages

Au NCs are generally synthesized by a galvanic replacement reaction developed by Xia group in 2002.[18] Typically, silver nanocubes are prepared as a template by reducing silver nitrate with polyvinyl pyrolidone (PVP) at an elevated temperature. PVP also serves as capping agents and the reaction solvent. The size of the silver nanocubes is controlled by the amount of silver nitrate, with increased amount of silver ions for nanocages of larger sizes. To the purified silver nanocube solution, hydrogen tetrachloroaurate was injected at the boiling temperature. The auric acid is reduced to gold atoms by the silver nanoparticles due to higher standard reduction potential of gold than silver. The gold atoms epitaxially nucleate on the silver nanocube and then grow into a thin shell around the silver

template. The fact that it takes three silver atoms to reduce one gold atom creates the hole in the cubes as the wall of the empty cube becomes gold leading to a hollow structure having gold walls. With holes in them the wall thickness and the size of holes of the Au NCs are controlled by the amount of gold salt. Increasing the amount of gold salt produces nanocages with thinner shells and porous walls.

4. Therapeutic applications

4.1. Gold nanospheres

PPTT involving contrast agents of gold-based nanoparticles was reported for the first time by Lin and co-workers in 2003 using gold nanospheres in combination with a nanosecond visible pulsed laser.[33] Anti-CD8 immunogold nanoparticles specifically bound to T lymphocyte cells and subsequent irradiation with laser pulses lead to destruction of over 90%. Of the cells, visible PPTT of cancer cells using gold nanoparticles and pulsed laser has been extensively investigated later by Zharov et al.[34] It was found that cell death could be induced by a single nanosecond pulse at an energy of 2–3 J/cm^2 with 10–15 gold nanoparticles per cell. Visible PPTT of cancer cells using gold nanoparticles was later been studied by El-Sayed group using a continuous argon ion laser.[35] By using a numerical model, the group found that a temperature around 75 °C was reached in the cells for cell death by the laser heating of gold nanoparticles on the cells.[36] Visible PPTT can be used for fundamental in vitro studies, but its practical applications in in vivo are limited as visible light does not penetrate tissue optimally. For in vivo and clinical therapy of tumors under skin and deeply seated within tissue, NIR light is required because of its deep penetration due to minimal absorption of the hemoglobin and water molecules in tissues in this spectral region. Thus, NIR-absorbing plasmonic nanoparticles are favored in PPTT of cancer.

4.2. Gold nanoshells

NIR PPTT of cancer using gold-based nanoparticles was firstly developed by Halas and co-workers using Au NSs in 2003.[37] Au NSs were prepared and stabilized with poly (ethylene) glycol (PEG). In the presence of PEG-coated Au NSs, breast cancer cells were destroyed after exposure to cw NIR light at an intensity of 35 w/cm^2 for 7 min (Fig. 3A). Using a mouse model, they demonstrated that breast cancer xenografted tumors were destroyed after Au NSs intratumoral injection and NIR laser irradiation for a few minutes (Fig. 3B). MRI showed a temperature rise of 37 °C. Subsequent studies showed complete tumor eradication at 10 days post-treatment.[38] They also showed that 55% of the mice receiving NS therapy/laser treatment experienced complete tumor regression without regrowth after 90 days.[39] The NSs exhibit a blood half-life time about 4 h and are dominantly accumulated in mouse liver and spleen. They also found that the nanoparticles started to clear out of body after 6 months. Their other research on NIR PPTT using Au NSs can be found in their recent review.[40]

4.3. Gold nanorods

NIR PPTT using gold nanorods was firstly demonstrated by El-Sayed group in 2006 through in vitro studies.[41] The NRs are functionalized with anti-EGFR antibodies for specific binding to EGFR-positive human oral cancer cells. After exposure to a beam of focused NIR light, the cancer cells were destroyed without affecting the normal cells (Fig. 4A and B). The method has also been demonstrated on some other cell types by other researchers.[42,43] Two years later, the group demonstrated the feasibility of PEGylated Au NRs for tumor photothermal ablation using a human oral cancer xenograft mouse model.[44] NIR imaging located the tumors due to the light absorption of the NRs that were treated either intravenously or intratumorally (Fig. 4C). Tumor growth was significantly inhibited ($p < 0.05$) after exposure to a low dose of NIR light (1–2 W/cm^2, 10–15 min) for the NR-treated groups (Fig. 4D). Thermal transient measurements showed that the temperature increased by over 20° is sufficient to induce tumor tissue destruction. Very recently, Bhatia and co-workers showed that single intravenous injection of PEGylated Au NRs enables complete eradication of all irradiated tumors in mice without regrowth over 50 days.[45] They also conducted a quantitative comparison of the photothermal effects between Au NSs and NRs. Their results show that NRs generate heat over six times faster than NSs per gram of gold. They have a

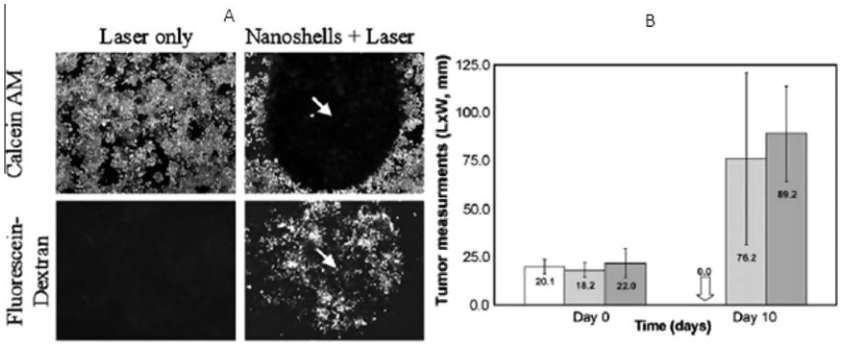

Figure 3 NIR PPTT using Au NSs. (A) In vitro PPTT; (B) in vivo tumor PPTT. Blank: NSs and laser treatment; Gray: shame treatment; Dark: untreated controls. While laser itself does not affect the cell viability, the treatment of Au NSs induces cell death within the laser irradiation area at a laser intensity of 37 W/cm^2. Tumors are completely ablated for the NSs and laser treated groups, but not shame and control groups. (A) Reproduced with permission from Hirsch et al.[37]; (B) reproduced with permission from O'Neal et al.[38]

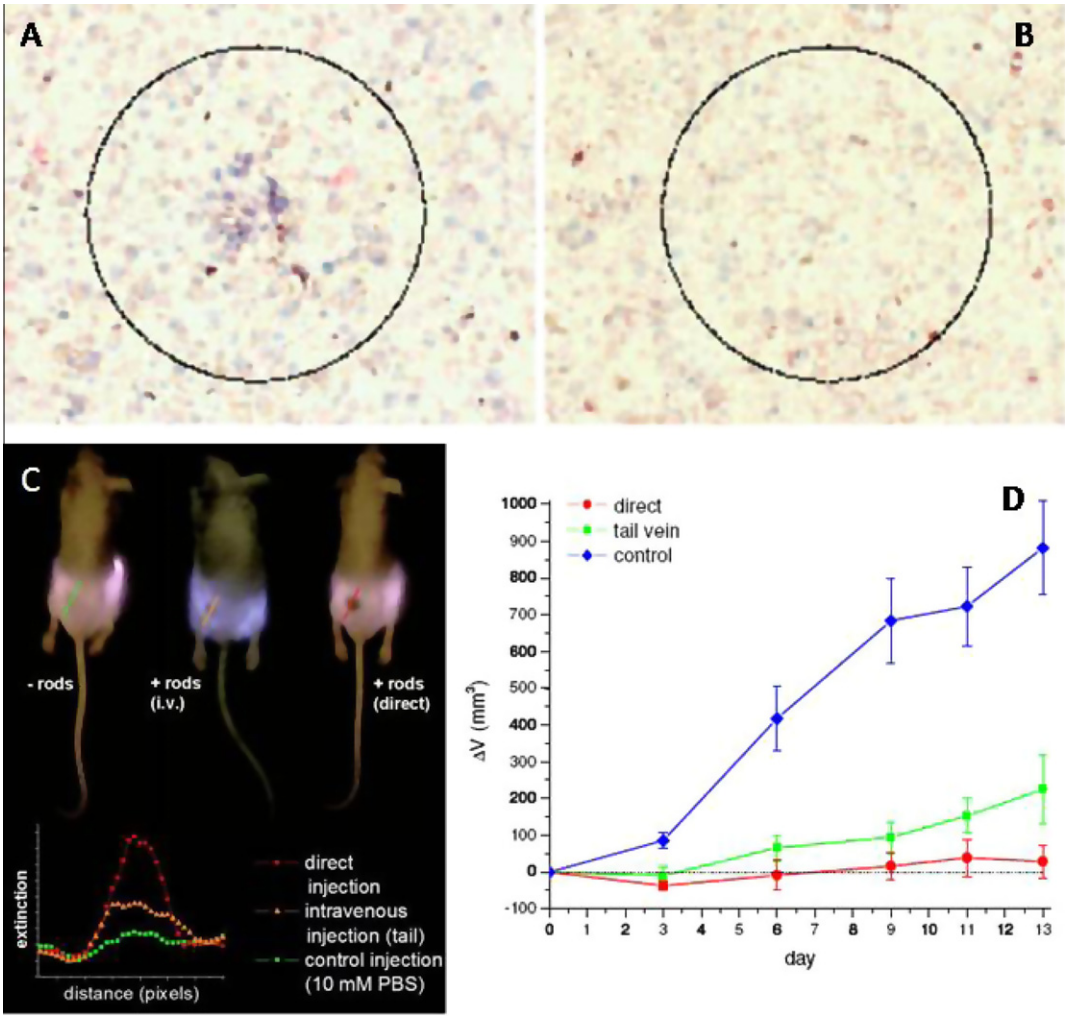

Figure 4 NIR PPTT using Au NRs. (A and B) Selective in vitro photothermal cancer therapy; (C and D) in vivo NIR tumor imaging and PPTT therapy. At 10 W/cm^2, the cancer cells within the laser spot undergo irreversible photodestruction (A) while the normal cells are not affected (B). The tumors are identified by a black spot under NIR illumination due to the light absorption by the nanorods that are administrated into the tumor either intratumorally or intravenously. NIR irradiation of the nanorod treated tumors leads to significant inhibition of the tumor growth rate compared to control tumors. (A and B) Reproduced with permission from Huang et al.[41]; (C and D) reprinted with permission from Dickerson et al.[44]

blood half life time around 17 h, which is superior long compared to Au NSs.

4.4. Gold nanocages

In 2007, Xia and co-workers demonstrated the feasibility of Au NCs for NIR PPTT in vitro (Fig. 5A and B).[46] The NCs ere conjugated with anti-HER2 antibodies to target HER2 on breast cancer cells. Cell destruction was observed at a laser power density of 1.5–4.7 W/cm^2. They also found that the cell circulation damage area is linearly dependent on the laser power density. The cell death efficiency increases with increasing laser exposure time until steady state at 5 min.[47] The in vivo nanoparticle active targeting and biodistribution of Au NCs have been considerably studied by Li and co-workers[48] using anti-EGFR conjugated Au NCs and 111. In-labeling, they show that the NCs reach tumor at 6.8% ID/g. Targeted PPTT of melanoma xenografted tumors on mice was studied by the same group using the ligand of α-melanocyte-stimulating hormone (MSH) analog that target melanocortin type-1receptor overexpressed in melanoma.[49] The tumor affinity of targeted NCs is about three times of that of the non-targeted ones. Photothermal studies show that tumor uptake of [18F] fluorodeoxyglucose, indicating reduced metabolic activity after laser treatment. In contrast, there are no significant changes on the metabolic activity of tumors for non-targeted and saline ones. Histologic examination also shows that 66% of tumor tissues show necrotic response for targeted NCs but only 7.9% were observed for the tumors treated with the non-targeted NCs and saline solution (Fig. 5C). These quantitative studies are very important on the evaluation of PPTT outcomes.

5. Cell death mechanisms

Photothermally induced cell death can take place via apoptosis or necrosis depending on the laser dosage, type and irradiation time. It also depends on the subcellular location of the

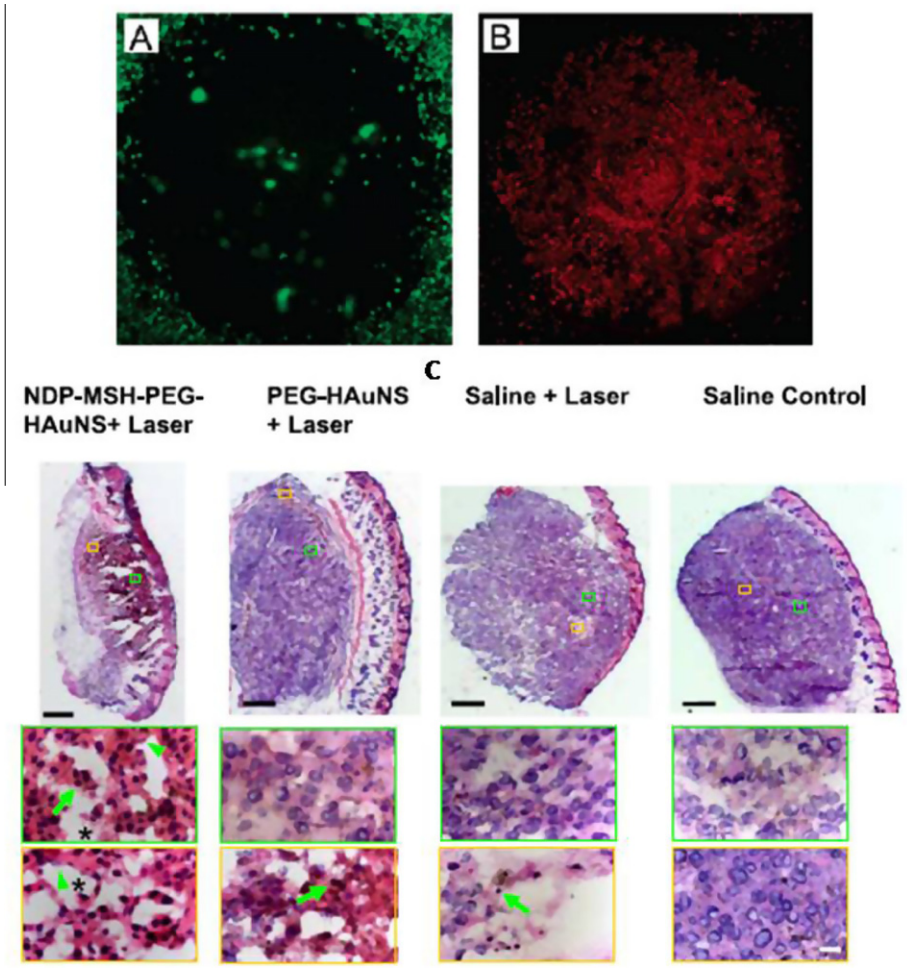

Figure 5 NIR PPTT using Au NCs. (A and B) In vitro PPTT; (C) in vivo tumor tissue destruction assessed by histologic staining. Only for the active targeted and laser treated tumors, tumor cells show extensive pyknosis (arrows), karyolysis (arrowheads), cytoplasmic acidophilia, and degradation of the extracellular matrix of the tumor (asterisks). (A and B) Reproduced with permission from Chen et al.[46]; (C) reproduced with permission from Lu et al.[49]

nanoparticles. Cell death mechanisms have been explored to some degree. Under pulsed laser irradiation studied by Zharov and co-workers,[50] laser pulses could induce cell damage via a series of photothermal and accompanied phenomena; denaturation or breakdown of proteins, cell cavitation, cellular structure rupturing, evaporation of cellular liquid and bubble formation by shock waves due to particle thermal expansion, evaporation, optical breakdown or plasma generation of Au NPs. The photothermolysis mechanism of NIR PPTT with cw lasers and Au NRs has been elucidated in some degree by Wei and Cheng groups.[43] Their studies show that the laser energy used to destroy the cells when the nanoparticles are located on the cytoplasm membrane is 10 times lower than that required when the nanoparticles are internalized inside the cytoplasm. The energy required for a fs laser is 10 fold lower than that when a cw laser is used. Based on these results and staining of cell membrane integrity, cell viability and actin filaments, they found that cell death was initiated by the disruption of the plasma membrane. Subsequent influx of calcium ions induces membrane blebbing and damage of actin filaments. Obviously, apoptosis is the route of cell destruction by the laser heating of gold nanoparticles.

6. Future perpective

As nanotechnologists, we have devised methods to destroy cancer cells and thus stop cancer as a disease. In order to use a new medicine, we must make sure that it does not have side harmful effects. In most new medicines, this can take a long time. If the harmful effects can be eliminated using animal trials, the new medicine can be approved for human trials and if it works safely in humans, the new medicine can be approved. This is where the use of gold nanotechnology is at the moment. A great amount of detailed animal experiments are now going on at the Egyptian National Research Center and in the USA between the Winship Cancer of Emory University and our Nano-Technology group at Georgia Institute of Technology aimed at determining and trying to solve the toxicity of gold nanoparticles when injected in animals. If this can be accomplished, we hope to go for human trials. This will

take a long time that cannot be predicted as it depends on the results of a great deal of research.

References

1. Jemal A, Siegel R, Ward E, Hao Y, Xu J, Murray T, et al.. *Cancer J Clin* 2009;**59**:225.
2. Brunetaud JM, Mordon S, Maunoury V, Beacco C. *Lasers Med Sci* 1995;**10**:3–8.
3. Huang X, Jain PK, El-Sayed IH, El-Sayed MA. *Lasers Med Sci* 2008;**23**:217.
4. Huang X, Neretina S, El-Sayed MA. *Adv Mater* 2009;**21**:4880.
5. Mie G. *Ann Phys* 1908;**25**:377.
6. Jain PK, Lee KS, El-Sayed IH, El-Sayed MA. *J Phys Chem B* 2006;**110**:7238.
7. Loo CH, Lin A, Hirsch LR, Lee MH, Barton J, Halas NJ, et al.. *Technol Cancer Res Treat* 2004;**3**:33.
8. Hu M, Chen J, Li ZY, Au L, Hartland GV, Li X, et al.. *Chem Soc Rev* 2006;**35**:1084.
9. Neeves AE, Birnboim MH. *J Opt Soc Am B* 1989;**6**:787.
10. Oldenburg SJ, Averitt RD, Westcott SL, Halas NJ. *Chem Phys Lett* 1998;**288**:243.
11. Prodan E, Radloff C, Halas NJ, Nordlander P. *Science* 2003;**302**:419.
12. Jain PK, El-Sayed MA. *Nano Lett* 2007;**7**:2854.
13. Yu YY, Chang SS, Lee CL, Wang CRC. *J Phys Chem B* 1997;**101**:6661.
14. Jana NR, Gearheart L, Murphy CJ. *Adv Mater* 2001;**13**:1389.
15. Nikoobakht B, El-Sayed MA. *Chem Mater* 2003;**15**:1957.
16. Gans R. *Ann Phys* 1915;**47**:270.
17. Link S, Mohamed MB, El-Sayed MA. *J Phys Chem B* 1999;**103**:3073.
18. Sun Y, Mayers BT, Xia Y. *Nano Lett* 2002;**2**:481.
19. Chen J, Wiley B, Li ZY, Campbell D, Saeki F, Cang H, et al.. *Adv Mater* 2005;**17**:2255.
20. Link S, El-Sayed MA. *Ann Rev Phys Chem* 2003;**54**:331.
21. Faraday M. *Philos Trans* 1857;**147**:145.
22. Turkevich J, Stvenson PC, Hillier J. *Disc Farad Soc* 1951;**11**:55.
23. Frens G. *Nat Phys Sci* 1973;**241**:20.
24. Schmid G, Boese R, Pfeil R, Bandermann F, Meyer S, Calis GHM, et al.. *Chem Ber* 1981;**114**:3634.
25. Brust M, Walker M, Bethell D, Schiffrin DJ, Whyman RJ. *J Chem Soc Chem Commun* 1994;801.
26. Jana NR, Gearheart L, Murphy C. *J Chem Mater* 2001;**13**:2313.
27. Foss Jr CA, Hornyak GL, Tierney MJ, Martin CR. *J Phys Chem* 1992;**96**:9001.
28. Torigoe K, Esumi K. *Langmuir* 1992;**8**:59.
29. Xin F, Gui Y, Zheng X. *Wuji Huaxue Xuebao* 2005;**21**:822.
30. Kim YJ, Cho G, Song JH. *Nuclear Instrum Meth Phys Res B* 2006;**246**:351.
31. Liu FK, Chang YC, Ko FH, Chu TC. *Mater Lett* 2003;**58**:373.
32. Cao J, Ma X, Zheng M, Liu J, Ji H. *Chem Lett* 2005;**34**:730.
33. Pitsillides CM, Joe EK, Wei X, Anderson RR, Lin CP. *Biophys J* 2003;**84**:4023.
34. Zharov VP, Kim JW, Curiel DT, Everts M. *Nanomed Nanotechnol Biol Med* 2005;**1**:326.
35. El-Sayed IH, Huang X, El-Sayed MA. *Cancer Lett* 2006;**239**: 129.
36. Huang X, Jain PK, El-Sayed IH, El-Sayed MA. *Photochem Photobiol* 2006;**82**:412.
37. Hirsch LR, Stafford RJ, Bankson JA, Sershen SR, Price RE, Hazle JD, et al.. *Proc Natl Acad Sci USA* 2003;**100**:13549.
38. O'Neal DP, Hirsch LR, Halas NJ, Payne JD, West JL. *Cancer Lett* 2004;**209**:171.
39. James WD, Hirsch LR, West JL, O'Neal PD, Payne JD. *J Radioanal Nucl Chem* 2007;**271**:455.
40. Lal S, Clare SE, Halas NJ. *Acc Chem Res* 2008;**41**:1842.
41. Huang X, El-Sayed IH, Qian W, El-Sayed MA. *J Am Chem Soc* 2006;**128**:2115.
42. Takahashi H, Niidome T, Nariai A, Niidome Y, Yamada S. *Chem Lett* 2006;**35**:500.
43. Tong L, Zhao Y, Huff TB, Hansen MN, Wei A, Cheng JX. *Adv Mater* 2007;**19**:3136.
44. Dickerson EB, Dreaden EC, Huang X, El-Sayed IH, Chu H, Pushpanketh S, et al.. *Cancer Lett* 2008;**269**:57.
45. von Maltzahn G, Park JH, Agrawal A, Bandaru NK, Das SK, Sailor MJ, et al.. *Cancer Res* 2009;**69**:3892.
46. Chen J, Wang D, Xi J, Au L, Siekkinen A, Warsen A, et al.. *Nano Lett* 2007;**7**:1318.
47. Au L, Zheng D, Zhou F, Li ZY, Li X, Xia Y. *ACS Nano* 2008;**2**:1645.
48. Melancon MP, Lu W, Yang Z, Zhang R, Cheng Z, Elliot AM, et al.. *Mol Cancer Ther* 2008;**7**:1730.
49. Lu W, Xiong C, Zhang G, Huang Q, Zhang R, Zhang JZ, et al.. *Clin Cancer Res* 2009;**15**:876.
50. Pustovalov VK, Smetannikov AS, Zharov VP. *Laser Phys Lett* 2008;1.